

EMBOMATRIX: A SCALABLE TRAINING-GROUND FOR EMBODIED DECISION-MAKING

Zixing Lei^{1,2}, Sheng Yin¹, Yichen Xiong¹, Yuanzhuo Ding¹, Wenhao Huang¹, Yuxi Wei¹,
Qingyao Xu¹, Yiming Li³, Weixin Li², Yunhong Wang², and Siheng Chen¹

¹Shanghai Jiao Tong University, ²Zhongguancun Academy, ³New York University

ABSTRACT

Embodied decision-making enables agents to translate high-level goals into executable actions through continuous interactions within the physical world, forming a cornerstone of general-purpose embodied intelligence. Large language models (LLMs), with their general decision-making capabilities, offer a promising path to realize this potential; however, LLMs trained solely on language lack exposure to physical environments, limiting their true embodied understanding. To bridge this gap, we propose the concept of a **training ground**: a comprehensive infrastructure that provides task and scene simulation, embodied interaction, and feedback signals, offering a one-stop solution for LLM acquire genuine embodied decision-making skills. In this work, we present **EmboMatrix**, the first training ground of its kind, providing massive and diverse tasks with efficient simulation and precise rewards. EmboMatrix incorporates a series of novel techniques: a multi-agent data engine for large-scale task and scene generation, a distributed heterogeneous-hardware system for scalable simulation, and a multi-level reward architecture for precise supervision. Leveraging EmboMatrix, we cultivate **EmboBrain**, an LLM whose embodied decision-making abilities emerge from extensive embodied interactions. Experiments show that EmboBrain-7B surpasses the 671B DeepSeek-R1 baseline by 9.5% on two challenging embodied decision-making benchmarks, demonstrating the power of interactive, environment-grounded learning for building truly intelligent embodied agents. Code will be released in <https://github.com/EmboMaster/EmboMatrix>.

1 INTRODUCTION

Embodied decision-making (Li et al., 2024c) enables agents to translate high-level goals into executable actions through continuous interactions with the physical world, forming the cornerstone of general-purpose embodied intelligence. Without it, agents can hardly generalize across diverse tasks or operate effectively in complex, dynamic scenarios. Existing efforts largely follow two paradigms. End-to-end Vision-Language-Action (VLA) Kim et al. (2025) models map raw sensory inputs directly to low-level motor commands, implicitly performing embodied decision-making by integrating perception and action to achieve high-level goals, but they require vast imitation data and struggle with long-horizon planning. Hierarchical approaches Birr et al. (2024); Li et al. (2024b); Driess et al. (2023); Brohan et al. (2023); Mu et al. (2023); Wang et al. (2023a); Wu et al. (2023); Wang et al. (2023c) decouple high-level reasoning from low-level control: low-level models execute primitive skills, while a high-level model orchestrates embodied decision-making by interpreting instructions, reasoning about the world, and decomposing tasks into actionable sub-goals. This structure simplifies long-horizon reasoning and allows integration of advanced models, such as large language models, into the decision-making loop. In this work, we adopt the hierarchical paradigm and focus on enhancing the high-level model’s embodied decision-making to enable robust, generalizable, and adaptive behavior across diverse tasks.

Large language models (LLMs), with their advanced reasoning and general decision-making abilities, offer a promising foundation for embodied decision-making. Early work (Li et al., 2024c) demonstrated the

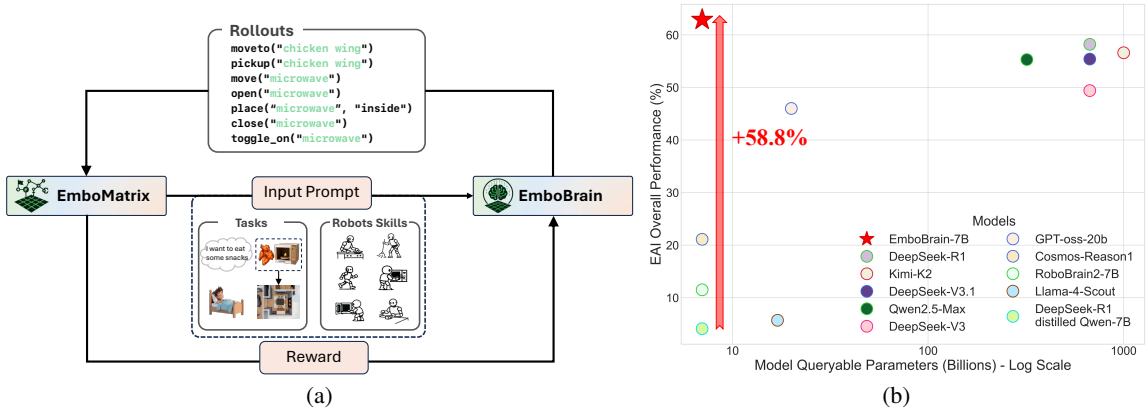


Figure 1: **EmboMatrix → EmboBrain: overview and empirical gains.** (a) **Overall idea.** EmboMatrix composes an *input prompt* from task goals and a library of robot skills, which conditions EmboBrain to generate executable rollouts (e.g., `moveto`, `pickup`, `open`, `toggle_on`). Execution in the environment returns a reward, closing the loop and enabling prompt adaptation and policy learning. (b) **Effect.** On the *Embodied Agent Interface* benchmark, EmboMatrix-augmented training boosts a 7B base model by **+58.8** percentage points in success rate, outperforming domain-specialized baselines and even much larger LLMs.

zero-shot competence of LLMs on curated datasets. Some subsequent studies (Azzolini et al., 2025; Ji et al., 2025) enhanced these abilities through fine-tuning on specialized datasets, such as physically grounded question-answering pairs, injecting curated embodied knowledge. Although convenient, such non-interactive fine-tuning resembles a “brain in a vat”: it promotes rote memorization rather than true understanding of physical dynamics, and the resulting gains are often limited even with large amounts of training data. Achieving genuine mastery in embodied decision-making requires interactive learning, which involves acting, perceiving feedback, and adapting. However, direct training in the real world is costly, risky, and difficult to scale. This motivates the use of **high-fidelity simulation environments**, which replicate physical dynamics, enable efficient and large-scale interaction, and provide rich feedback, allowing agents to safely acquire and refine the skills needed for robust, real-world decision-making.

To enable genuine embodied decision-making, we introduce the concept of a **training ground**: a comprehensive infrastructure that provides task and scene simulation, realistic embodied interaction, and feedback signals, allowing models to acquire embodied decision-making skills through trial-and-error in physically grounded environments. Constructing such a training ground is highly challenging due to the inherent complexity of the embodied domain. At the data level, it requires generating a massive, diverse, and scalable curriculum of tasks that are both physically plausible and guaranteed to be solvable. At the system level, no existing simulation platform can support the high-throughput, large-scale interactions necessary to train high-capacity LLMs effectively. At the algorithmic level, it demands the design of an informative reward architecture tailored to embodied scenarios, providing dense supervision while avoiding the biases and limitations of manual reward engineering. Together, these technical challenges make the construction of a high-level training ground a complex and demanding task.

To this end, we introduce **EmboMatrix**, the first training ground designed for embodied decision-making, enabling high-throughput interaction and efficient training with massive and diverse tasks and scenes. EmboMatrix offers three key advantages: (i) **Data diversity**: a multi-agent driven automated data factory generates large numbers of tasks, enabling models to acquire generalizable capabilities across varied environments; (ii) **System scalability**: compatibility with distributed, heterogeneous hardware, combined with semantic abstraction and pre-caching of low-level processes, substantially improves simulation throughput; and (iii) **Informative supervision**: a hierarchical reward architecture delivers richer learning signals for embodied

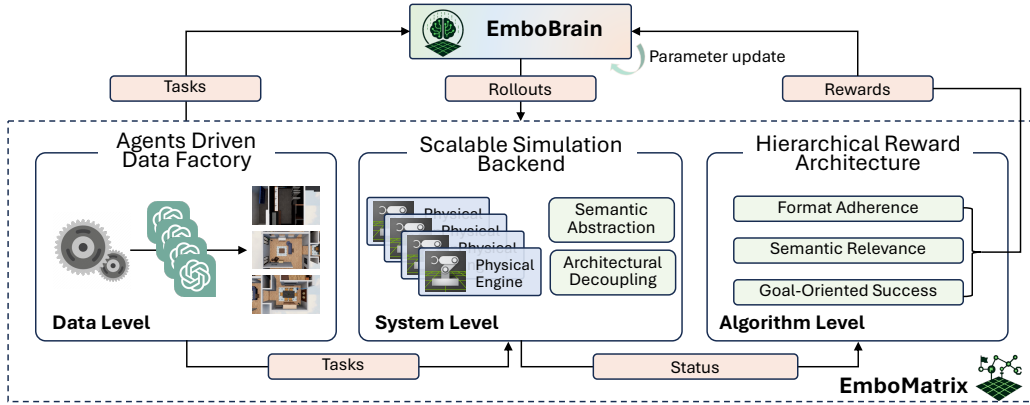


Figure 2: Overview of the *EmboMatrix* training pipeline.

decision-making. Compared with conventional robot simulators, EmboMatrix provides a one-stop solution for embodied decision-making: it not only supports simulation of richer and more diverse scenarios, but also automatically generates physically grounded tasks and enables large-scale model training, resulting in substantially higher training efficiency and broader generalization.

Leveraging EmboMatrix, we train **EmboBrain**, an LLM whose embodied decision-making abilities emerge from extensive interaction within the training ground. This process effectively transforms a purely language-trained model into a truly embodied agent capable of perceiving, acting, and adapting in physical environments. Experiments show that EmboBrain-7B achieves substantial gains on multiple challenging embodied decision-making benchmarks, surpassing the strong DeepSeek-R1 baseline by 9.5% on average. These results demonstrate that interactive, environment-grounded learning, powered by a comprehensive training ground, is a transformative path toward building truly intelligent embodied agents.

2 RELATED WORK

Embodied Decision Making. LLM are used to generate text based action sequences directly Driess et al. (2023); Brohan et al. (2023); Mu et al. (2023); Wang et al. (2023a); Wu et al. (2023); Wang et al. (2023c); translate instructions into executable code Liang et al. (2022); Singh et al. (2022); or provide intermediate representations consumed by downstream modules Jiang et al. (2022); Dalal et al. (2024). Knowledge-augmented variants improve grounding via dynamic memory Ding et al. (2023); Hazra et al. (2023); Li et al. (2024d); Chen et al. (2024). Reactive embodied agents combine LLM reasoning with online adaptation Birr et al. (2024); Tian et al. (2024); Liang et al. (2024). Additional work addresses anomaly detection, zero-shot knowledge extraction, and physics reasoning Sinha et al. (2024); Huang et al. (2022); Hao et al. (2023).

Simulator and Embodied Data Generation. Recent benchmarks have expanded simulation for embodied agent, yet most—e.g., Behavior1K Li et al. (2024a), VirtualHome Puig et al. (2018), ALFRED Shridhar et al. (2020), iGibsonXia et al. (2020), Meta-World Yu et al. (2021), RLBench James et al. (2019), Habitat Szot et al. (2022), BEHAVIOR Srivastava et al. (2021), robosuite Zhu et al. (2025), TDW Transport Gan et al. (2021), SAPIEN Xiang et al. (2020), ManiSkill Mu et al. (2021); Gu et al. (2023), RFUniverse Fu et al. (2023), SoftGym Lin et al. (2021), and EmbodiedBench Yang et al. (2025)—depend on manual scene authoring, limiting scale and diversity. Tools such as ProcTHOR Deitke et al. (2022) broaden environments but remain rule-bound. Recent LLM- and diffusion-aided methods (HOLODECK Yang et al. (2024b), ARCHITECT Wang et al. (2024), DiffuScene Tang et al. (2024), WorldCraft Liu et al. (2025b)) generate visually rich scenes yet ignore task constraints or object interactions, while RoboGen Wang et al. (2023b) ties generation to small, simple layouts. A detailed comparation is shown in Tab 4. We address them with a multi-agent automated data factory that produces diverse, task-aware scenarios at scale.

RL for Large Language Models. LLM alignment via RL encompasses safety-aware feedback Dai et al. (2024); Lee et al. (2024); Chu et al. (2023), analyses of RLHF’s effects on generalization and diversity Rafailov et al. (2023); Kirk et al. (2024), improved reward modeling via Nash learning and uncertainty estimation Munos et al. (2024), and more sample-efficient optimizers such as GPO and GRPO Zhao et al. (2024); Liu et al. (2025a). However, a systematic framework for training embodied decision making with RL remains lacking, limiting progress toward grounded embodied decision-making in complex environments. The work most closely related to ours is Fei et al. (2025), which introduces RL post-training for embodied decision-making. In contrast, we concretely instantiate a physics-based simulation system, provide substantially larger-scale data, and design a more informative reward system tailored to embodied decision-making.

3 PROBLEM FORMULATION

Let \mathbf{B}_θ be a model for high-level embodied decision-making parameterized by learnable weights θ . Given a high-level instruction I , the current embodied scene S as input and predefined robots skills library \mathcal{A} , the action sequence \mathbf{a} in a physical space is then obtained as

$$\mathbf{a} = \mathbf{B}_\theta(S, I, \mathcal{A}), \quad \text{where } \mathbf{a} = (a_1, \dots, a_H) \text{ and } a_i \in \mathcal{A}. \quad (1)$$

This process is defined as **embodied decision-making**.

Consider a **training ground** cultivates such a embodied decision-making model. Mathematically, let $\mathcal{F}_{\mathcal{D}_{\text{task}}, \mathcal{M}, \mathcal{R}}(\cdot)$ be a training ground parameterized by a collection of embodied tasks $\mathcal{D}_{\text{task}}$, an interactive physical simulator \mathcal{M} , and a reward architecture \mathcal{R} . Here an embodied task set $\mathcal{D}_{\text{task}} = \{T_i\}_{i=1}^N$ has N tasks, where $T_i = (S_i, I_i, \mathcal{G}_i)$ is the i th tasks with S_i , the configuration that instantiates the scene in the simulator, containing all task-relevant objects and their initial states, I_i , the high-level instruction of T_i (e.g. heat sandwich) and \mathcal{G}_i , the target conditions by binding them to concrete assets (e.g., sandwich inside microwave).

Let \mathbf{B}_{θ_0} be an input base model. Then, the optimized embodied decision-making model is obtained as

$$\mathbf{B}_{\theta^*} = \mathcal{F}_{\mathcal{D}_{\text{task}}, \mathcal{M}, \mathcal{R}}(\mathbf{B}_{\theta_0}). \quad (2)$$

The optimization objective is to find the optimal parameters θ^* by maximizing the expected reward across this task distribution:

$$\theta^* = \arg \max_{\theta} \mathbb{E}_{T \sim \mathcal{D}_{\text{task}}} [\mathcal{R}(\mathcal{M}(T, \mathbf{B}_\theta(S, I, \mathcal{A})))], \quad (3)$$

In this work, our proposed system, **EmboMatrix**, is the concrete realization of the training ground $\mathcal{F}_{\mathcal{D}_{\text{task}}, \mathcal{M}, \mathcal{R}}(\cdot)$, which will be described in Section 4.

4 METHODS

The preceding section established that enhancing an agent’s embodied decision-making capability requires a comprehensive **training ground**. In this chapter, we introduce **EmboMatrix**, which operates as a system to continuously improve an agent’s capabilities of embodied decision-making. As shown in Figure 2, the entire training process is orchestrated by EmboMatrix. The cycle begins at the Data Level, where our agents driven data factory procedurally generates a diverse tasks set. This task is presented to the models, which produces a action sequence rollout. The action sequence is then executed at the System Level by our Scalable Simulation Backend, which leverages a high-fidelity physical engine to produce the final environments status for the action sequences. Finally, at the Algorithm Level, our hierarchical reward architecture evaluates this final environments status. This reward signal drives the parameter update for the EmboBrain, completing the learning loop. The following sections will detail the design of each of these three synergistic components.

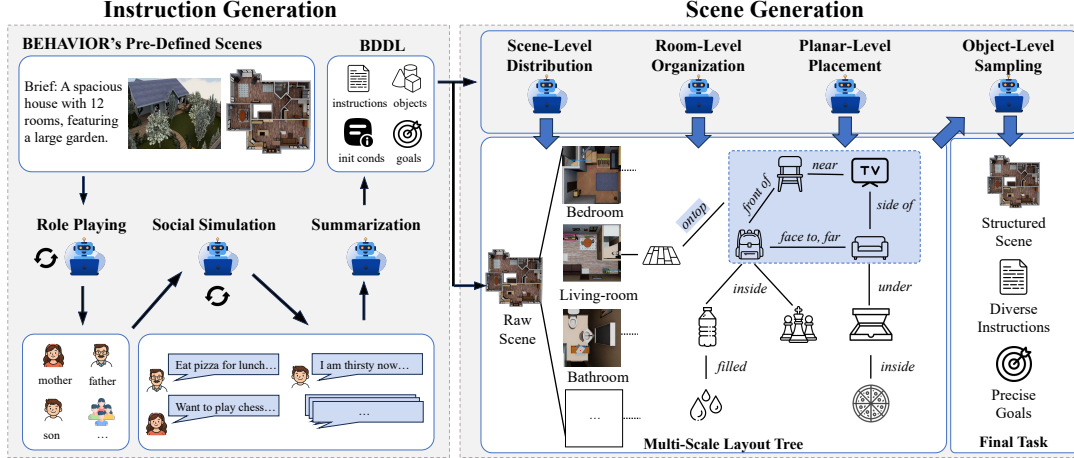


Figure 3: Pipeline of Multi-Agent-Driven Automated Data Factory.

4.1 MULTI-AGENT-DRIVEN AUTOMATED DATA FACTORY.

Multi-agent social simulation for instruction generation. Since generating one task amounts to producing $(\mathcal{S}, \mathcal{I}, \mathcal{G})$, we bootstrap from BEHAVIOR’s pre-defined scenes (e.g., hotel rooms, household interiors), yielding a base layout \mathcal{S}_0 with plausibly distributed asset states (Li et al., 2024a). To synthesize diverse and scene-faithful tasks, as shown in Fig 3, we employ a multi-agent social simulation module with role-playing (Tang et al., 2025; Li et al., 2023). The module first extracts information from \mathcal{S}_0 , renders RGB images from egocentric and top-down views, and prompts a VLM to distill a concise textual scene description. Socially simulated agents then generate relevant characters (e.g., *father*, *mother*, *child*, *home robot*) and conduct multi-round dialogues in which human agents articulate language-based needs for the embodied agent; the exchanges are iteratively refined until concrete requirements emerge. Each scene can be repeatedly simulated to create a large number of semantically diverse instructions \mathcal{I} . An LLM-based agent subsequently summarizes \mathcal{I} into a BDDL format (Li et al., 2022), which contains \mathcal{G} , \mathcal{O} , and \mathcal{IC} .

Multi-level scene generation. We further employ a multi-agent and multi-level scene generation module to efficiently and faithfully transform \mathcal{S}_0 into an instantiated scene \mathcal{S} . As shown in Fig 3, these agents allocate \mathcal{O} across different rooms, analyze the states of each room, and design a **multi-scale layout tree** such that object placement not only satisfies \mathcal{IC} but also ensures spatial plausibility and visual aesthetics. Beyond basic relations (e.g., *under*, *inside*), the tree refines specializations such as *ontop* (Yang et al., 2024a), while employing constraints like *faceto* and *insideof* to regulate object placement on the same plane with higher precision and consistency. Finally, sampling agents place objects in the simulator according to the tree structure, resulting in an executable task \mathcal{T} with a realistic and well-structured scene.

With this multi-agent–driven data factory, we can randomize across scenes and social simulations, thereby rapidly generating realistic and diverse tasks and laying a solid data foundation for subsequent training.

4.2 SCALABLE SIMULATION BACKEND

To facilitate the massive scale of interaction required by our learning objective in equation 3, the system architecture must overcome two fundamental hurdles: the computational cost of individual physical interactions and the systemic overhead of massively parallel execution. We address these through a principled approach of semantic abstraction and architectural decoupling.

Semantic Abstraction via a Pre-Cached Physics Interface. A primary performance bottleneck is the *granularity mismatch* between the LLM’s high-level semantic commands and the simulator’s computationally expensive, low-level micro-dynamics. To resolve this, our **pre-cached language-physics interface** acts as a semantic abstraction layer. For common interactions, instead of simulating the full physical process, we bypass the costly dynamics by directly instantiating a valid, physically plausible outcome from a pre-computed set of post-conditions. This outcome-based simulation approach dramatically accelerates throughput while preserving the semantic consequences crucial for the learning signal. See more details in Appendix B.

Architectural Decoupling for Massively Parallel Rollouts. A second challenge arises from the conflicting resource requirements of LLM training and large-scale physics simulation, which renders a monolithic architecture inefficient and unscalable. We resolve this by employing an architecturally decoupled, distributed simulation backend. This service-oriented design separates the LLM trainer from a heterogeneous pool of simulation workers, allowing each component to run on specialized, optimal hardware. However, this distributed architecture necessitates sophisticated scheduling to manage communication and I/O overheads. We address this with two key components: a **Resource-Scheduler** that predictively pre-loads future scenes onto idle workers to hide latency, and a **Task-Dispatcher** that maps incoming action sequences to these pre-warmed simulators to maximize utilization (details in Appendix B). This design resolves systemic resource conflicts and enables high-throughput rollouts at a scale unattainable by conventional approaches.

4.3 HIERARCHICAL REWARD ARCHITECTURE

A central challenge in applying RL to long-horizon embodied tasks is the severe credit assignment problem. A sparse, binary reward for final task completion provides insufficient guidance for meaningful exploration in a combinatorially large state-action space. To overcome this, we eschew a single, static reward function and instead introduce a **hierarchical reward architecture**. This architecture provides a dynamic, multi-stage curriculum of supervision signals designed to guide the agents from basic format adherence to complex, goal-oriented semantic reasoning. The total reward $r_i = r_f + r_r + r_g$ is composed of three tiers, each targeting a distinct stage of the learning process.

Format Adherence (r_f). The foundational stage of the curriculum focuses on teaching the agents to generate well-formed outputs. The agents receives a binary format reward, r_f , which provides a simple, rule-based signal for whether its output conforms to the prescribed action schema. As demonstrated in prior work (Wang et al., 2025; Shao et al., 2024), this initial phase of enforcing syntactic correctness is crucial for stabilizing early training and ensuring a high rate of executable rollouts.

Semantic Relevance (r_r). Once the agent can generate valid syntax, the curriculum shifts to guiding exploration. The relevance reward, r_r , serves as a dense, intermediate signal that bridges the gap between random exploration and goal-directed behavior. It is defined as:

$$r_r = \beta |\mathcal{O}_{\text{goal}} \cap \mathcal{O}_{\mathbf{a}}|, \quad \beta > 0,$$

where $\mathcal{O}_{\text{goal}}$ is the set of objects required to achieve the goal and $\mathcal{O}_{\mathbf{a}}$ is the set of unique objects the agent’s action sequence interacts with. By rewarding the agent for interacting with any goal-relevant object, r_r effectively shapes the agent’s behavior, encouraging it to focus its exploration on the semantically pertinent subset of the vast interaction space, even before it can successfully complete any sub-goals.

Goal-Oriented Success (r_g). The final tier of the curriculum provides the ground-truth signal for task completion. The goal reward, r_g , is a sum over the individual goal predicates defined by the task:

$$r_g = \alpha \sum_{g_k \in \mathcal{G}} \mathbb{I}[g_k(s_H) = 1], \quad \alpha > 0.$$

Table 1: Comprehensive comparison of model success rates (%) on two benchmarks: our agent-generated benchmark and the Embodied Agent Interface (EAI) benchmark. On our agent-generated benchmark, our model, **EmboBrain-7B**, outperforms GPT-4o and DeepSeek-R1 by 18.2 and 14.8 percentage points, respectively. Models are grouped into three categories: cells with  denote large-parameter models,  denote embodied-scene enhanced models, and  denote EmboBrain-related models.

| Model | Size | Our Agent-Generated Benchmark | | | | | Embody Agent Interface (EAI) Benchmark | | | | |
|-----------------------|------|-------------------------------|----------------|------------------|-------------------|---------------|--|----------------|------------------|-------------------|---------------|
| | | Overall | Pick and Place | Appliances Using | Kitchen Operation | Compound Task | Overall | Pick and Place | Appliances Using | Kitchen Operation | Compound Task |
| GPT-4o-mini | - | 12.0 | 17.2 | 13.4 | 6.5 | 15.1 | 26.5 | 43.5 | 27.1 | 8.1 | 21.7 |
| GPT-01-mini | - | 33.4 | 50.2 | 39.6 | 17.2 | 38.6 | 58.6 | 66.9 | 70.0 | 26.5 | 60.9 |
| GPT-4o | - | 45.0 | 45.9 | 43.8 | 38.1 | 55.6 | 44.8 | 62.2 | 58.0 | 22.3 | 37.6 |
| GPT-oss-20b | 20B | 20.6 | 27.6 | 27.5 | 9.2 | 26.7 | 46.0 | 60.6 | 45.0 | 35.4 | 40.6 |
| DeepSeek-V3 | 671B | 40.1 | 59.3 | 38.6 | 19.7 | 56.0 | 49.4 | 52.0 | 62.8 | 29.5 | 50.5 |
| DeepSeek-R1 | 671B | 51.6 | 67.1 | 56.1 | 36.6 | 58.7 | 58.2 | 61.8 | 79.5 | 32.0 | 58.6 |
| DeepSeek-V3.1 | 671B | 41.0 | 48.6 | 44.2 | 27.2 | 53.1 | 55.4 | 63.9 | 64.7 | 42.4 | 51.8 |
| Llama-4-Scout | 17B | 1.4 | 5.0 | 1.1 | 0.3 | 0.2 | 5.7 | 8.7 | 4.1 | 3.2 | 5.2 |
| Kimi-K2 | 1T | 48.5 | 52.1 | 47.2 | 41.7 | 56.8 | 56.6 | 62.2 | 68.4 | 34.6 | 57.0 |
| Qwen2.5-Max | 320B | 11.7 | 16.7 | 16.7 | 3.6 | 16.3 | 55.3 | 63.5 | 69.4 | 33.0 | 53.5 |
| RoboBrain2-7B | 7B | 20.9 | 26.0 | 22.2 | 18.5 | 19.1 | 11.5 | 12.6 | 17.3 | 6.7 | 10.8 |
| Cosmos-Reason1 | 7B | 5.9 | 7.9 | 7.8 | 4.0 | 5.7 | 21.1 | 21.7 | 25.9 | 14.4 | 21.7 |
| 1.5B Base | 1.5B | 3.8 | 4.8 | 2.8 | 0.9 | 8.4 | 0.2 | 0.1 | 0.1 | 0.0 | 0.3 |
| EmboBrain-1.5B | 1.5B | 48.7 | 54.8 | 47.2 | 44.1 | 51.4 | 8.9 | 8.2 | 7.7 | 7.2 | 10.3 |
| 7B Base | 7B | 5.5 | 11.9 | 5.6 | 2.7 | 14.6 | 4.1 | 1.0 | 4.9 | 1.3 | 6.8 |
| EmboBrain-7B | 7B | 65.8 | 73.2 | 62.7 | 60.1 | 70.3 | 62.9 | 75.6 | 70.0 | 37.7 | 61.4 |

The multi-level reward system ensures that, on the one hand, informative guidance is provided during the early stages of model training, while on the other hand, the goal achievement serves as the primary driver, preventing the model from falling into inductive bias.

4.4 LEARNING ALGORITHMS

We train the high-level embodied decision-making model with *Group Relative Policy Optimization* (GRPO) DeepSeek-AI et al. (2025). For every task–scene pair in a mini-batch we draw G complete action sequences $\{\mathbf{a}_{j,i}\}_{i=1}^G$ from the current policy, execute them once, and record the episode-level rewards $r_{j,i}$ defined in Section 4.3. **Group-Normalized Advantage.** Within each group j we compute the mean \bar{r}_j and standard deviation σ_j , then form the advantage $A_{j,i} = \frac{r_{j,i} - \bar{r}_j}{\sigma_j}$.

GRPO Surrogate Objective.

Let $\rho_{j,i} = \mathbf{B}_\theta(\mathbf{a}_{j,i}) / \mathbf{B}_{\theta_{\text{old}}}(\mathbf{a}_{j,i})$. The policy is updated by maximising

$$\mathcal{L}_{\text{GRPO}} = \frac{1}{BG} \sum_{j=1}^B \sum_{i=1}^G \min(\rho_{j,i} A_{j,i}, \text{clip}(\rho_{j,i}, 1 - \varepsilon, 1 + \varepsilon) A_{j,i}) - \beta D_{\text{KL}}[\mathbf{B}_\theta \parallel \mathbf{B}_{\text{ref}}],$$

where ε is the clipping parameter and β is the KL weight with respect to the reference model π_{ref} .

5 EXPERIMENTS

In this section, we present a comprehensive experiments designed to validate the efficacy of the **EmboMatrix** framework. Our evaluation is structured to answer three major questions, which directly correspond to the data, system, and algorithmic challenges addressed in this work:

| Task: Heat chicken | | |
|--|---|--|
| GPT-4o: score 0 move("chicken wing") pickup("chicken wing") move("microwave") Forget open toggle_on("microwave") microwave cook("chicken wing", "heat") move("table") place("chicken wing", "ontop", "table") | DeepSeek-R1: score 0.5 move("chicken wing") pickup("chicken wing") move("microwave") Forget toggle_on open("microwave") microwave place("microwave", "inside") close("microwave") cook("chicken wing", "heat") | EmboBrain 7B Model: score 1 move("chicken wing") pickup("chicken wing") move("microwave") Correct open("microwave") place("microwave", "inside") close("microwave") toggle_on("microwave") |
| | | |

Figure 4: Qualitative comparison on the *Heat Chicken* task. GPT-4o omits opening the microwave door; DeepSeek-R1 inserts the food but never toggles the appliance on; only our EmboBrain-7B produces a complete, executable sequence and succeeds in simulation.

1. **EmboMatrix Effectiveness:** Does end-to-end training within the EmboMatrix framework substantially improve the performance of different LLMs on complex, long-horizon embodied decision-making tasks?
2. **EmboMatrix Scalability:** Do the data and system components of EmboMatrix deliver the requisite diversity and throughput to support scalable, long-term training? Specifically, we analyze the diversity of our procedurally generated tasks and the efficiency of our distributed simulation backend.
3. **Algorithmic Efficiency:** How effective is our hierarchical reward architecture at improving sample efficiency and overall learning outcomes compared to simpler, baseline reward schemes?

5.1 OVERALL PERFORMANCE ON EMBODIED DECISION-MAKING

We begin by addressing our first question: to what extent does end-to-end training within the **EmboMatrix** framework improve the performance of LLMs on complex embodied tasks? To this end, we train our models and evaluate them on two challenging benchmarks, demonstrating significant performance gains.

Experimental Setup. We train two models, denoted **EmboBrain-1.5B** and **EmboBrain-7B**. These models are initialized from the publicly available DeepSeek-R1 distilled Qwen-1.5B and 7B checkpoints (referred to as “1.5B base and 7B base” in table 1),, respectively, and are subsequently trained within our **EmboMatrix** framework using the GRPO algorithm. The input prompt provided to the model at each decision step comprises four key components: a predefined task description, a profile of the agent’s capabilities, a simulator-generated description of the current scene state, and a formatting instruction for the output. LLM optimization ran on an $8 \times$ A100 cluster, while parallel simulation was executed on a pool of 16 graphics GPU. The training dataset for our models is entirely procedurally generated by our Multi-Agent-Driven Automated Task Factory. This process leverages a base set of 45 diverse scenes from the Behavior-1K environment (Li et al., 2024a) to synthesize a large-scale training corpus. For evaluation, we assess model performance on two distinct, held-out benchmarks, each containing 100 challenging task-scene pairs: First, **Internal-Verified**: A manually verified test set generated by our own pipeline to ensure high-quality and challenging scenarios. Second, **Embody Agent Interface (EAI) Benchmark**: a published benchmark for embodied decision-making based on behavior dataset (Li et al., 2024c). All tasks are categorized into four representative types: (1) *Pick and Place*, involving basic object manipulation and organization; (2) *Appliance Usage*, requiring the agent to change the state of household devices; (3) *Kitchen Operations*, including food-related tasks such as heating or freezing; and (4) *Compound Tasks*, which consist of multi-step instructions spanning multiple categories.

Results. We compare our models with representative proprietary and open-source LLMs with well-accepted leading performance. To reduce sampling variance, each model is queried ten times per task, and we report the average result for each pair. Table 1 summarizes the outcomes and highlights key observations: (i) Physical interaction training with **EmboMatrix** significantly enhances the embodied decision-making capabilities of general-purpose LLMs. Specifically, for 1.5B model, EmboMatrix improve its performance by 44.9% and 8.7%, for 7B model, EmboMatrix improve its performance by 60.3% and 58.8%, respectively, in two benchmarks. The 1.5B model exhibits relative limited performance on the EAI benchmark constrained by the

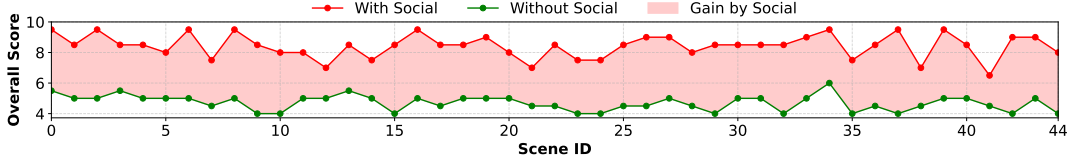


Figure 5: Social simulation significantly increases the diversity of tasks.

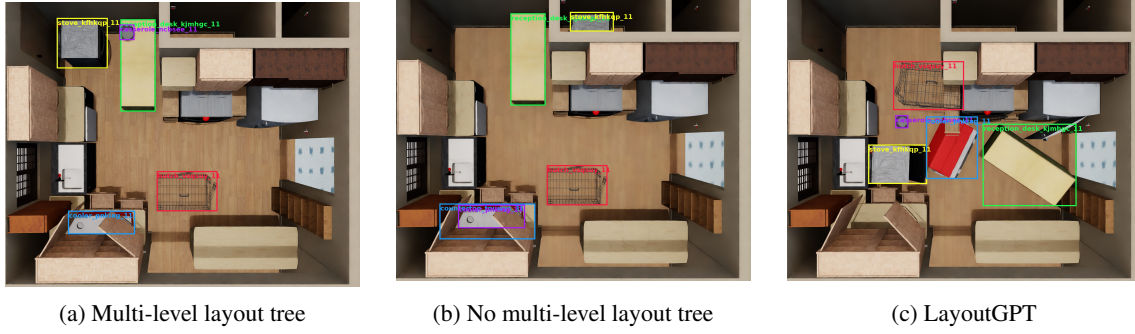


Figure 6: Multi-level layout tree significantly improves the aesthetics of scene generation.

capabilities of base model. (ii) Post-training with **EmboMatrix** enables a 7B model to outperform much larger models, including the proprietary GPT-4o and the 671B-parameter DeepSeek-R1 on both embodied decision-making tasks. (iii) The largest gains are observed in the most challenging category, Kitchen Operation, indicating that physically grounded learning is particularly beneficial for complex, multi-step reasoning.

Figure 4 compares roll-outs for the *Heat Chicken* task. All three models GPT-4o, DeepSeek-R1, and our EmboBrain-7B produce seemingly reasonable action sequences, yet only our model completes the task in simulation. GPT-4o omits opening the microwave door before place the chicken; DeepSeek-R1 places the food correctly but never toggle on. In contrast, EmboBrain-7B executes the full sequence: open door, insert food, close door, power on—and therefore succeeds. This example illustrates that action sequences appearing valid in text may still fail in physical environments, underscoring the importance of interaction in physical environments.

5.2 SCALABILITY OF EMBOMATRIX.

5.2.1 DATA DIVERSITY AND QUALITY.

Experimental Setup. We conduct two ablation studies focusing on task diversity and scene quality. First, to assess **task diversity**, we compare our social simulation-based approach against a direct generation baseline. For 45 scenes from behavior-1k, we generate 10 tasks with each method and use a GPT-4 evaluator to score the resulting diversity (details in Tab.6). Second, to evaluate **scene quality**, we compare our multi-level layout tree against two baselines (Omnigibson’s built-in functions and LayoutGPT Feng et al. (2023)) on 140 tasks. We measure performance across four metrics: generation success rate, time, verification pass rate, and scene aesthetics, with the latter also scored by a GPT-4 evaluator (details in Tab.7).

Table 2: Multi-level layout tree significantly improves the quality of scene generation.

| Method | Generation Rate | Aesthetic Score | Verification Pass Rate |
|-----------|-----------------|-----------------|------------------------|
| W/o Tree | 49.29 | 7.30 | 47.83 |
| LayoutGPT | 45.72 | 7.22 | 25.00 |
| Our | 71.43 | 8.11 | 98.00 |

Social Simulation Enhances Task Diversity. As shown in Fig. 5, incorporating social simulation significantly increases task diversity, achieving an average score of 8.42, compared to 4.70 without social simulation. Examples are provided in Tab. 5. **Multi-level Layout Tree Improves Scene Generation Quality.** Quantitative results in Tab. 2 show that the multi-level layout tree achieves the highest scene generation rate (71.43%) and verification pass rate (98.00%). Failures result from limited space or unmet task conditions. Without the layout tree, unstructured placements, such as positioning a bag before the table, lead to misalignments, reducing the generation rate to 49.29%. The absence of pre-checks for feasible robot positions also decreases the pass rate. LayoutGPT performs worst due to limited spatial reasoning, causing cluttered room layouts. Scenes with the layout tree also achieve the highest aesthetics score (8.11), while those generated by other methods often miss key objects, place them incorrectly, or result in cluttered layouts, as shown in Fig. 5.

5.2.2 SIMULATION EFFICIENCY SUPPORT TRAINING PROCESS.

Table 3 presents an ablation study validating our system’s efficiency by measuring the average per-rollout simulation latency. A naive implementation exhibits a high latency of 3.48s. By progressively enabling our three key optimizations—**Pre-cached Execution**, a predictive **Resource Scheduler**, and a **Task Dispatcher**, our full system achieves a final latency of just **0.07s**. This nearly 50-fold reduction in overhead is critical, providing the massive simulation throughput required for our large-scale reinforcement learning experiments.

5.3 HIERARCHICAL REWARD ARCHITECTURE IMPROVE TRAINING EFFICIENCY

To validate the effectiveness of our hierarchical reward architecture, we conduct an ablation study on the impact of the semantic relevance reward (r_r). As illustrated in Figure 7, the learning curves demonstrate a stark difference in training efficiency and final performance. The agent trained without the semantic relevance reward makes minimal progress, stagnating at a low goal-oriented success reward. This indicates that without this intermediate guidance, the agent is unable to solve the credit assignment problem and discover a successful policy in a sparse-reward setting. In contrast, the agent trained with the semantic relevance reward exhibits a rapid and stable increase in performance, achieving a significantly higher final reward. This result confirms that semantic relevance reward is a critical component of our training ground’s design, enabling efficient learning by providing a dense and meaningful signal that effectively guides the agent’s exploration towards goal-oriented behaviors.

6 CONCLUSION

Conclusion. In this work, we argue for a paradigm shift from learning language data to interactive learning for embodied agents. We introduced **EmboMatrix**, the first scalable **training ground** that makes this vision practical by addressing the challenges of data, system, and algorithm design. Our framework successfully transforms general-purpose Large Language Models into powerful **EmboBrain** models, with our EmboBrain-7B achieving a 14.2% performance gain over a strong baseline. EmboMatrix provides a complete and validated solution for the continuous improvement of embodied agents through direct, simulated experience.

Table 3: Abalation of efficiency. Latency measures the average time to simulate a scenario. We reduces this overhead by over 50x.

| Pre-cached Execution | Resource Scheduler | Task Dispatcher | Latency (s) |
|----------------------|--------------------|-----------------|-------------|
| | | | 3.48 |
| ✓ | | | 0.85 |
| ✓ | ✓ | | 0.14 |
| ✓ | ✓ | ✓ | 0.07 |

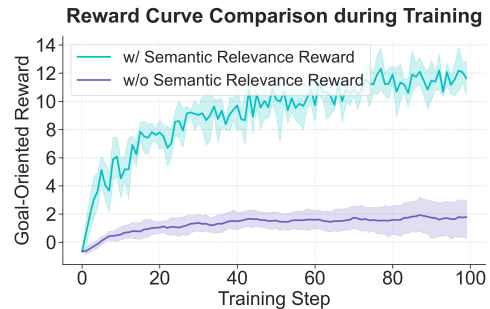


Figure 7: Effect of semantic relevance reward.

REFERENCES

Alisson G. Azzolini, Hannah Brandon, Prithvijit Chattopadhyay, Huayu Chen, Jinju Chu, Yin Cui, Jenna Diamond, Yifan Ding, Francesco Ferroni, Rama Govindaraju, Jinwei Gu, Siddharth Gururani, El Hanafi, Imad, Zekun Hao, Huffman, Jacob Samuel, Jingyi Jin, Brendan Johnson, Rizwan Khan, George Kurian, Elena Lantz, Nayeon Lee, Li, Zhaoshuo, Xuan Li, Tsung-Yi Lin, Yen-Chen Lin, Ming-Yu Liu, Alice Luo, Andrew Mathau, Yun Ni, Lindsey Pavao, Wei Ping, David W. Romero, Misha Smelyanskiy, Shuran Song, Lyne Tchapmi, Andrew Z. Wang, Boxin Wang, Haoxiang Wang, Fangyin Wei, Jiashu Xu, Yao Xu, Xiaodong Yang, Zhuolin Yang, Xiaohui Zeng, and Zhe Zhang. *Cosmos-reason1: From physical common sense to embodied reasoning*. *CoRR*, abs/2503.15558, 2025. doi: 10.48550/ARXIV.2503.15558. URL <https://doi.org/10.48550/arXiv.2503.15558>.

Timo Birr, Christoph Pohl, Abdelrahman Younes, and Tamim Asfour. Autogpt+p: Affordance-based task planning with large language models. *arXiv preprint arXiv:2402.10778*, 2024.

Anthony Brohan, Noah Brown, Justice Carbajal, et al. Rt-2: Vision-language-action models transfer web knowledge to robotic control. In *Conference on Robot Learning*, pp. 2165–2183, 2023.

Yongchao Chen, Jacob Arkin, Yilun Hao, Yang Zhang, Nicholas Roy, and Chuchu Fan. Prompt optimization in multi-step tasks (promst): Integrating human feedback and preference alignment. *ArXiv*, abs/2402.08702, 2024. URL <https://api.semanticscholar.org/CorpusID:267657588>.

Kun Chu, Xufeng Zhao, Cornelius Weber, Mengdi Li, and Stefan Wermter. Accelerating reinforcement learning of robotic manipulations via feedback from large language models. *CoRR*, abs/2311.02379, 2023. doi: 10.48550/ARXIV.2311.02379. URL <https://doi.org/10.48550/arXiv.2311.02379>.

Josef Dai, Xuehai Pan, Ruiyang Sun, Jiaming Ji, Xinbo Xu, Mickel Liu, Yizhou Wang, and Yaodong Yang. Safe RLHF: safe reinforcement learning from human feedback. In *The Twelfth International Conference on Learning Representations, ICLR 2024, Vienna, Austria, May 7-11, 2024*. OpenReview.net, 2024. URL <https://openreview.net/forum?id=TyFrPOKYXw>.

Murtaza Dalal, Tarun Chiruvolu, Devendra Singh Chaplot, and Ruslan Salakhutdinov. Plan-seq-learn: Language model guided rl for solving long horizon robotics tasks. In *ICLR*, 2024.

DeepSeek-AI, Daya Guo, Dejian Yang, Haowei Zhang, Junxiao Song, Ruoyu Zhang, Runxin Xu, Qihao Zhu, Shirong Ma, Peiyi Wang, Xiao Bi, Xiaokang Zhang, Xingkai Yu, Yu Wu, Z. F. Wu, Zhibin Gou, Zhihong Shao, Zhuoshu Li, Ziyi Gao, Aixin Liu, Bing Xue, Bingxuan Wang, Bochao Wu, Bei Feng, Chengda Lu, Chenggang Zhao, Chengqi Deng, Chenyu Zhang, Chong Ruan, Damai Dai, Deli Chen, Dongjie Ji, Erhang Li, Fangyun Lin, Fucong Dai, Fuli Luo, Guangbo Hao, Guanting Chen, Guowei Li, H. Zhang, Han Bao, Hanwei Xu, Haocheng Wang, Honghui Ding, Huajian Xin, Huazuo Gao, Hui Qu, Hui Li, Jianzhong Guo, Jiashi Li, Jiawei Wang, Jingchang Chen, Jingyang Yuan, Junjie Qiu, Junlong Li, J. L. Cai, Jiaqi Ni, Jian Liang, Jin Chen, Kai Dong, Kai Hu, Kaige Gao, Kang Guan, Kexin Huang, Kuai Yu, Lean Wang, Lecong Zhang, Liang Zhao, Litong Wang, Liyue Zhang, Lei Xu, Leyi Xia, Mingchuan Zhang, Minghua Zhang, Minghui Tang, Meng Li, Miaojun Wang, Mingming Li, Ning Tian, Panpan Huang, Peng Zhang, Qiancheng Wang, Qinyu Chen, Qiushi Du, Ruiqi Ge, Ruisong Zhang, Ruizhe Pan, Runji Wang, R. J. Chen, R. L. Jin, Ruyi Chen, Shanghao Lu, Shangyan Zhou, Shanhua Chen, Shengfeng Ye, Shiyu Wang, Shuiping Yu, Shunfeng Zhou, Shuting Pan, and S. S. Li. Deepseek-r1: Incentivizing reasoning capability in llms via reinforcement learning. *DeepSeek Technical Report*, abs/2501.12948, 2025. doi: 10.48550/ARXIV.2501.12948. URL <https://doi.org/10.48550/arXiv.2501.12948>.

Matt Deitke, Eli VanderBilt, Alvaro Herrasti, Luca Weihs, Kiana Ehsani, Jordi Salvador, Winson Han, Eric Kolve, Aniruddha Kembhavi, and Roozbeh Mottaghi. Procthor: Large-scale embodied ai using procedural generation. *Advances in Neural Information Processing Systems*, 35:5982–5994, 2022.

Yan Ding, Xiaohan Zhang, Chris Paxton, and Shiqi Zhang. Task and motion planning with large language models for object rearrangement. *2023 IEEE/RSJ International Conference on Intelligent Robots and Systems (IROS)*, pp. 2086–2092, 2023. URL <https://api.semanticscholar.org/CorpusID:257496672>.

Danny Driess, Fei Xia, Mehdi S. M. Sajjadi, Corey Lynch, Aakanksha Chowdhery, Brian Ichter, Ayzaan Wahid, Jonathan Tompson, Quan Vuong, Tianhe Yu, Wenlong Huang, Yevgen Chebotar, Pierre Sermanet, Daniel Duckworth, Sergey Levine, Vincent Vanhoucke, Karol Hausman, Marc Toussaint, Klaus Greff, Andy Zeng, Igor Mordatch, and Pete Florence. Palm-e: An embodied multimodal language model. In Andreas Krause, Emma Brunskill, Kyunghyun Cho, Barbara Engelhardt, Sivan Sabato, and Jonathan Scarlett (eds.), *International Conference on Machine Learning, ICML 2023, 23-29 July 2023, Honolulu, Hawaii, USA*, volume 202 of *Proceedings of Machine Learning Research*, pp. 8469–8488. PMLR, 2023. URL <https://proceedings.mlr.press/v202/driess23a.html>.

Zhaoye Fei, Li Ji, Siyin Wang, Junhao Shi, Jingjing Gong, and Xipeng Qiu. Unleashing embodied task planning ability in llms via reinforcement learning. *arXiv preprint arXiv:2506.23127*, 2025.

Weixi Feng, Wanrong Zhu, Tsu jui Fu, Varun Jampani, Arjun Akula, Xuehai He, Sugato Basu, Xin Eric Wang, and William Yang Wang. Layoutpt: Compositional visual planning and generation with large language models, 2023. URL <https://arxiv.org/abs/2305.15393>.

Haoyuan Fu, Wenqiang Xu, Ruolin Ye, Han Xue, Zhenjun Yu, Tutian Tang, Yutong Li, Wenxin Du, Jieyi Zhang, and Cewu Lu. Rfuniverse: A multiphysics simulation platform for embodied ai, 2023. URL <https://arxiv.org/abs/2202.00199>.

Chuang Gan, Siyuan Zhou, Jeremy Schwartz, Seth Alter, Abhishek Bhandwaldar, Dan Gutfreund, Daniel L. K. Yamins, James J DiCarlo, Josh McDermott, Antonio Torralba, and Joshua B. Tenenbaum. The threeworld transport challenge: A visually guided task-and-motion planning benchmark for physically realistic embodied ai, 2021. URL <https://arxiv.org/abs/2103.14025>.

Jiayuan Gu, Fanbo Xiang, Xuanlin Li, Zhan Ling, Xiqiang Liu, Tongzhou Mu, Yihe Tang, Stone Tao, Xinyue Wei, Yunchao Yao, Xiaodi Yuan, Pengwei Xie, Zhiao Huang, Rui Chen, and Hao Su. Maniskill2: A unified benchmark for generalizable manipulation skills, 2023. URL <https://arxiv.org/abs/2302.04659>.

Shibo Hao, Yi Gu, Haodi Ma, Joshua Jiahua Hong, Zhen Wang, Daisy Zhe Wang, and Zhiting Hu. Reasoning with language model is planning with world model. *ArXiv*, abs/2305.14992, 2023. URL <https://api.semanticscholar.org/CorpusID:258865812>.

Rishi Hazra, Pedro Zuidberg Dos Martires, and Luc De Raedt. Saycanpay: Heuristic planning with large language models using learnable domain knowledge. *ArXiv*, abs/2308.12682, 2023. URL <https://api.semanticscholar.org/CorpusID:261100610>.

Wenlong Huang, Pieter Abbeel, Deepak Pathak, and Igor Mordatch. Language models as zero-shot planners: Extracting actionable knowledge for embodied agents. *arXiv preprint arXiv:2201.07207*, 2022.

Stephen James, Zicong Ma, David Rovick Arrojo, and Andrew J. Davison. Rlbench: The robot learning benchmark & learning environment, 2019. URL <https://arxiv.org/abs/1909.12271>.

Yuheng Ji, Huajie Tan, Jiayu Shi, Xiaoshuai Hao, Yuan Zhang, Hengyuan Zhang, Pengwei Wang, Mengdi Zhao, Yao Mu, Pengju An, Xinda Xue, Qinghang Su, Huaihai Lyu, Xiaolong Zheng, Jiaming Liu, Zhongyuan Wang, and Shanghang Zhang. Robobrain: A unified brain model for robotic manipulation from abstract to concrete. *CoRR*, abs/2502.21257, 2025. URL <https://doi.org/10.48550/arXiv.2502.21257>.

Yunfan Jiang, Agrim Gupta, Zichen Zhang, et al. Vima: General robot manipulation with multimodal prompts. In *Advances in Neural Information Processing Systems*, volume 35, pp. 29917–29930, 2022.

Moo Jin Kim, Karl Pertsch, Siddharth Karamchetti, Ted Xiao, Ashwin Balakrishna, Suraj Nair, Rafael Rafailov, Ethan P Foster, Pannag R Sanketi, Quan Vuong, et al. Openvla: An open-source vision-language-action model. In *Conference on Robot Learning*, pp. 2679–2713. PMLR, 2025.

Robert Kirk, Ishita Mediratta, Christoforos Nalmpantis, Jelena Luketina, Eric Hambo, Edward Grefenstette, and Roberta Raileanu. Understanding the effects of RLHF on LLM generalisation and diversity. In *The Twelfth International Conference on Learning Representations, ICLR 2024, Vienna, Austria, May 7-11, 2024*. OpenReview.net, 2024. URL <https://openreview.net/forum?id=PXD3FAVHJT>.

Harrison Lee, Samrat Phatale, Hassan Mansoor, Thomas Mesnard, Johan Ferret, Kellie Lu, Colton Bishop, Ethan Hall, Victor Carbune, Abhinav Rastogi, and Sushant Prakash. RLAIF vs. RLHF: scaling reinforcement learning from human feedback with AI feedback. In *Forty-first International Conference on Machine Learning, ICML 2024, Vienna, Austria, July 21-27, 2024*. OpenReview.net, 2024. URL <https://openreview.net/forum?id=uydQ2W41KO>.

Chengshu Li, Fei Xia, Roberto Martín-Martín, Michael Lingelbach, Sanjana Srivastava, Bokui Shen, Kent Elliott Vainio, Cem Gokmen, Gokul Dharan, Tanish Jain, et al. igibson 2.0: Object-centric simulation for robot learning of everyday household tasks. In *Conference on Robot Learning*, pp. 455–465. PMLR, 2022.

Chengshu Li, Ruohan Zhang, Josiah Wong, Cem Gokmen, Sanjana Srivastava, Roberto Martín-Martín, Chen Wang, Gabrael Levine, Wensi Ai, Benjamin Jose Martinez, Hang Yin, Michael Lingelbach, Minjune Hwang, Ayano Hiranaka, Sujay Garlanka, Arman Aydin, Sharon Lee, Jiankai Sun, Mona Anvari, Manasi Sharma, Dhruba Bansal, Samuel Hunter, Kyu-Young Kim, Alan Lou, Caleb R. Matthews, Ivan Villa-Renteria, Jerry Huayang Tang, Claire Tang, Fei Xia, Yunzhu Li, Silvio Savarese, Hyowon Gweon, C. Karen Liu, Jiajun Wu, and Li Fei-Fei. BEHAVIOR-1K: A human-centered, embodied AI benchmark with 1, 000 everyday activities and realistic simulation. *CoRR*, abs/2403.09227, 2024a. doi: 10.48550/ARXIV.2403.09227. URL <https://doi.org/10.48550/arXiv.2403.09227>.

Guohao Li, Hasan Abed Al Kader Hammoud, Hani Itani, Dmitrii Khizbulin, and Bernard Ghanem. Camel: Communicative agents for "mind" exploration of large language model society. In *Thirty-seventh Conference on Neural Information Processing Systems*, 2023.

Manling Li, Shiyu Zhao, Qineng Wang, Kangrui Wang, Yu Zhou, Sanjana Srivastava, Cem Gokmen, Tony Lee, Li Erran Li, Ruohan Zhang, Weiyu Liu, Percy Liang, Li Fei-Fei, Jiayuan Mao, and Jiajun Wu. Embodied agent interface: Benchmarking llms for embodied decision making. In Amir Globersons, Lester Mackey, Danielle Belgrave, Angela Fan, Ulrich Paquet, Jakub M. Tomczak, and Cheng Zhang (eds.), *Advances in Neural Information Processing Systems 38: Annual Conference on Neural Information Processing Systems 2024, NeurIPS 2024, Vancouver, BC, Canada, December 10 - 15, 2024*, 2024b. URL http://papers.nips.cc/paper_files/paper/2024/hash/b631da756d1573c24c9ba9c702fde5a9-Abstract-Datasets_and_Benchmarks_Track.html.

Manling Li, Shiyu Zhao, Qineng Wang, Kangrui Wang, Yu Zhou, Sanjana Srivastava, Cem Gokmen, Tony Lee, Li, Li Erran, Ruohan Zhang, Weiyu Liu, Percy Liang, Fei-Fei, Li, Jiayuan Mao, and Jiajun Wu. Embodied agent interface: Benchmarking llms for embodied decision making. *CoRR*, abs/2410.07166, 2024c. URL <https://doi.org/10.48550/arXiv.2410.07166>.

Zhaoyi Li, Kelin Yu, Shuo Cheng, and Danfei Xu. LEAGUE++: EMPOWERING CONTINUAL ROBOT LEARNING THROUGH GUIDED SKILL ACQUISITION WITH LARGE LANGUAGE MODELS. In *ICLR 2024 Workshop on Large Language Model (LLM) Agents*, 2024d. URL <https://openreview.net/forum?id=xXo4JL8FvV>.

Jacky Liang, Wenlong Huang, Fei Xia, et al. Code as policies: Language model programs for embodied control. In *Advances in Neural Information Processing Systems*, volume 35, pp. 29218–29230, 2022.

Jacky Liang, Fei Xia, Wenhao Yu, Andy Zeng, Montse Gonzalez Arenas, Maria Attarian, Maria Bauza, Matthew Bennice, Alex Bewley, Adil Dostmohamed, Chuyuan Fu, Nimrod Gileadi, Marissa Giustina, Keerthana Gopalakrishnan, Leonard Hasenclever, Jan Humplik, Jasmine Hsu, Nikhil Joshi, Ben Jyenis, Chase Kew, Sean Kirmani, Tsang-Wei Edward Lee, Kuang-Huei Lee, Assaf Hurwitz Michaely, Joss Moore, Kenneth Oslund, Dushyant Rao, Allen Z. Ren, Baruch Tabanpour, Quan Ho Vuong, Ayzaan Wahid, Ted Xiao, Ying Xu, Vincent Zhuang, Peng Xu, Erik Frey, Ken Caluwaerts, Ting-Yu Zhang, Brian Ichter, Jonathan Tompson, Leila Takayama, Vincent Vanhoucke, Izhak Shafran, Maja Mataric, Dorsa Sadigh, Nicolas Manfred Otto Heess, Kanishka Rao, Nik Stewart, Jie Tan, and Carolina Parada. Learning to learn faster from human feedback with language model predictive control. *ArXiv*, abs/2402.11450, 2024. URL <https://api.semanticscholar.org/CorpusID:267751232>.

Xingyu Lin, Yufei Wang, Jake Olkin, and David Held. Softgym: Benchmarking deep reinforcement learning for deformable object manipulation, 2021. URL <https://arxiv.org/abs/2011.07215>.

Jie Liu, Gongye Liu, Jiajun Liang, Yangguang Li, Jiaheng Liu, Xintao Wang, Pengfei Wan, Di Zhang, and Wanli Ouyang. Flow-grpo: Training flow matching models via online rl, 2025a. URL <https://arxiv.org/abs/2505.05470>.

Xinhang Liu, Chi-Keung Tang, and Yu-Wing Tai. Worldcraft: Photo-realistic 3d world creation and customization via llm agents, 2025b. URL <https://arxiv.org/abs/2502.15601>.

Tongzhou Mu, Zhan Ling, Fanbo Xiang, Derek Yang, Xuanlin Li, Stone Tao, Zhiao Huang, Zhiwei Jia, and Hao Su. Maniskill: Generalizable manipulation skill benchmark with large-scale demonstrations, 2021. URL <https://arxiv.org/abs/2107.14483>.

Yuxiang Mu, Yuxin Liu, Jialu Zhang, et al. Embodiedgpt: Vision-language pre-training via embodied chain of thought. In *Advances in Neural Information Processing Systems*, volume 36, 2023.

Rémi Munos, Michal Valko, Daniele Calandriello, Mohammad Gheshlaghi Azar, Mark Rowland, Zhaohan Daniel Guo, Yunhao Tang, Matthieu Geist, Thomas Mesnard, Côme Fiebel, Andrea Michi, Marco Selvi, Sertan Girgin, Nikola Momchev, Olivier Bachem, Daniel J. Mankowitz, Doina Precup, and Bilel Piot. Nash learning from human feedback. In *Forty-first International Conference on Machine Learning, ICML 2024, Vienna, Austria, July 21-27, 2024*. OpenReview.net, 2024. URL <https://openreview.net/forum?id=Y5AmNYiyCQ>.

Xavier Puig, Kevin Ra, Marko Boben, Jiaman Li, Tingwu Wang, Sanja Fidler, and Antonio Torralba. Virtualhome: Simulating household activities via programs, 2018. URL <https://arxiv.org/abs/1806.07011>.

Rafael Rafailov, Archit Sharma, Eric Mitchell, Christopher D. Manning, Stefano Ermon, and Chelsea Finn. Direct preference optimization: Your language model is secretly a reward model. In Alice Oh, Tristan Naumann, Amir Globerson, Kate Saenko, Moritz Hardt, and Sergey Levine (eds.), *Advances in Neural Information Processing Systems 36: Annual Conference on Neural Information Processing Systems 2023, NeurIPS 2023, New Orleans, LA, USA, December 10 - 16, 2023*, 2023. URL http://papers.nips.cc/paper_files/paper/2023/hash/a85b405ed65c6477a4fe8302b5e06ce7-Abstract-Conference.html.

Zhihong Shao, Peiyi Wang, Qihao Zhu, Runxin Xu, Junxiao Song, Xiao Bi, Haowei Zhang, Mingchuan Zhang, Li, Y. K., Wu, Y., and Daya Guo. Deepseekmath: Pushing the limits of mathematical reasoning in open language models. *CoRR*, abs/2402.03300, 2024. URL <https://doi.org/10.48550/arXiv.2402.03300>.

Mohit Shridhar, Jesse Thomason, Daniel Gordon, Yonatan Bisk, Winson Han, Roozbeh Mottaghi, Luke Zettlemoyer, and Dieter Fox. Alfred: A benchmark for interpreting grounded instructions for everyday tasks, 2020. URL <https://arxiv.org/abs/1912.01734>.

Ishika Singh, Valts Blukis, Arsalan Mousavian, Ankit Goyal, Danfei Xu, Jonathan Tremblay, Dieter Fox, Jesse Thomason, and Animesh Garg. Progprompt: Generating situated robot task plans using large language models. *2023 IEEE International Conference on Robotics and Automation (ICRA)*, pp. 11523–11530, 2022. URL <https://api.semanticscholar.org/CorpusID:252519594>.

Rohan Sinha, Amine Elhafsi, Christopher Agia, et al. Real-time anomaly detection and reactive planning with large language models. In *Robotics: Science and Systems*, 2024.

Sanjana Srivastava, Chengshu Li, Michael Lingelbach, Roberto Martín-Martín, Fei Xia, Kent Vainio, Zheng Lian, Cem Gokmen, Shyamal Buch, C. Karen Liu, Silvio Savarese, Hyowon Gweon, Jiajun Wu, and Li Fei-Fei. Behavior: Benchmark for everyday household activities in virtual, interactive, and ecological environments, 2021. URL <https://arxiv.org/abs/2108.03332>.

Andrew Szot, Alex Clegg, Eric Undersander, Erik Wijmans, Yili Zhao, John Turner, Noah Maestre, Mustafa Mukadam, Devendra Chaplot, Oleksandr MakSYMets, Aaron Gokaslan, Vladimir Vondrus, Sameer Dharur, Franziska Meier, Wojciech Galuba, Angel Chang, Zsolt Kira, Vladlen Koltun, Jitendra Malik, Manolis Savva, and Dhruv Batra. Habitat 2.0: Training home assistants to rearrange their habitat, 2022. URL <https://arxiv.org/abs/2106.14405>.

Jiapeng Tang, Yinyu Nie, Lev Markhasin, Angela Dai, Justus Thies, and Matthias Nießner. Diffuscene: Denoising diffusion models for generative indoor scene synthesis, 2024. URL <https://arxiv.org/abs/2303.14207>.

Shuo Tang, Xianghe Pang, Zexi Liu, Bohan Tang, Rui Ye, Tian Jin, Xiaowen Dong, Yanfeng Wang, and Siheng Chen. Synthesizing post-training data for ILMs through multi-agent simulation. In Wanxiang Che, Joyce Nabende, Ekaterina Shutova, and Mohammad Taher Pilehvar (eds.), *Proceedings of the 63rd Annual Meeting of the Association for Computational Linguistics (Volume 1: Long Papers), ACL 2025, Vienna, Austria, July 27 - August 1, 2025*, pp. 23306–23335. Association for Computational Linguistics, 2025. URL <https://aclanthology.org/2025.acl-long.1136/>.

Xiaoyu Tian, Junru Gu, Bailin Li, et al. Drivevlm: The convergence of autonomous driving and large vision-language models. *arXiv preprint arXiv:2402.12289*, 2024.

Guanzhi Wang, Yuqi Xie, Yunfan Jiang, Ajay Mandlekar, Chaowei Xiao, Yuke Zhu, Linxi (Jim) Fan, and Anima Anandkumar. Voyager: An open-ended embodied agent with large language models. *ArXiv*, abs/2305.16291, 2023a. URL <https://api.semanticscholar.org/CorpusID:258887849>.

Yian Wang, Xiaowen Qiu, Jiageng Liu, Zhehuan Chen, Jiting Cai, Yufei Wang, Tsun-Hsuan Wang, Zhou Xian, and Chuang Gan. Architect: Generating vivid and interactive 3d scenes with hierarchical 2d inpainting. *arXiv preprint arXiv:2411.09823*, 2024.

Yiping Wang, Qing Yang, Zhiyuan Zeng, Liliang Ren, Lucas Liu, Baolin Peng, Hao Cheng, Xuehai He, Kuan Wang, Jianfeng Gao, Weizhu Chen, Shuohang Wang, Simon Shaolei Du, and Yelong Shen. Reinforcement learning for reasoning in large language models with one training example. *CoRR*, abs/2504.20571, 2025. URL <https://doi.org/10.48550/arXiv.2504.20571>.

Yufei Wang, Zhou Xian, Feng Chen, Tsun-Hsuan Wang, Yian Wang, Katerina Fragkiadaki, Zackory Erickson, David Held, and Chuang Gan. Robogen: Towards unleashing infinite data for automated robot learning via generative simulation. *arXiv preprint arXiv:2311.01455*, 2023b.

Zihao Wang, Shaofei Cai, Guanzhou Chen, Anji Liu, Xiaojian Ma, and Yitao Liang. Describe, explain, plan and select: Interactive planning with large language models enables open-world multi-task agents. *arXiv preprint arXiv:2302.01560*, 2023c.

Zhenyu Wu, Ziwei Wang, Xiuwei Xu, Jiwen Lu, and Haibin Yan. Embodied task planning with large language models. *ArXiv*, abs/2307.01848, 2023. URL <https://api.semanticscholar.org/CorpusID:259342896>.

Fei Xia, William B. Shen, Chengshu Li, Priya Kasimbeg, Micael Edmond Tchapmi, Alexander Toshev, Roberto Martin-Martin, and Silvio Savarese. Interactive gibson benchmark: A benchmark for interactive navigation in cluttered environments. *IEEE Robotics and Automation Letters*, 5(2):713–720, April 2020. ISSN 2377-3774. doi: 10.1109/LRA.2020.2965078. URL <http://dx.doi.org/10.1109/LRA.2020.2965078>.

Fanbo Xiang, Yuzhe Qin, Kaichun Mo, Yikuan Xia, Hao Zhu, Fangchen Liu, Minghua Liu, Hanxiao Jiang, Yifu Yuan, He Wang, Li Yi, Angel X. Chang, Leonidas J. Guibas, and Hao Su. Sapien: A simulated part-based interactive environment, 2020. URL <https://arxiv.org/abs/2003.08515>.

Rui Yang, Hanyang Chen, Junyu Zhang, Mark Zhao, Cheng Qian, Kangrui Wang, Qineng Wang, Teja Venkat Koripella, Marziyeh Movahedi, Manling Li, Heng Ji, Huan Zhang, and Tong Zhang. Embodiedbench: Comprehensive benchmarking multi-modal large language models for vision-driven embodied agents, 2025. URL <https://arxiv.org/abs/2502.09560>.

Yue Yang, Fan-Yun Sun, Luca Weihs, Eli VanderBilt, Alvaro Herrasti, Winson Han, Jiajun Wu, Nick Haber, Ranjay Krishna, Lingjie Liu, Chris Callison-Burch, Mark Yatskar, Aniruddha Kembhavi, and Christopher Clark. Holodeck: Language guided generation of 3d embodied ai environments. In *Proceedings of the IEEE/CVF Conference on Computer Vision and Pattern Recognition (CVPR)*, pp. 16227–16237, June 2024a.

Yue Yang, Fan-Yun Sun, Luca Weihs, Eli VanderBilt, Alvaro Herrasti, Winson Han, Jiajun Wu, Nick Haber, Ranjay Krishna, Lingjie Liu, et al. Holodeck: Language guided generation of 3d embodied ai environments. In *Proceedings of the IEEE/CVF Conference on Computer Vision and Pattern Recognition*, pp. 16227–16237, 2024b.

Tianhe Yu, Deirdre Quillen, Zhanpeng He, Ryan Julian, Avnish Narayan, Hayden Shively, Adithya Bellathur, Karol Hausman, Chelsea Finn, and Sergey Levine. Meta-world: A benchmark and evaluation for multi-task and meta reinforcement learning, 2021. URL <https://arxiv.org/abs/1910.10897>.

Siyan Zhao, John Dang, and Aditya Grover. Group preference optimization: Few-shot alignment of large language models. In *The Twelfth International Conference on Learning Representations, ICLR 2024, Vienna, Austria, May 7-11, 2024*. OpenReview.net, 2024. URL <https://openreview.net/forum?id=DpFeMH418Q>.

Yuke Zhu, Josiah Wong, Ajay Mandlekar, Roberto Martín-Martín, Abhishek Joshi, Kevin Lin, Abhiram Madukuri, Soroush Nasiriany, and Yifeng Zhu. robosuite: A modular simulation framework and benchmark for robot learning, 2025. URL <https://arxiv.org/abs/2009.12293>.

A DETAILED EXPLAINTION OF OUR MULTI-AGENT DATA FACTORY

Our multi-agent-driven automated data factory is designed to generate a vast and diverse set of realistic, long-horizon embodied AI tasks. The entire pipeline can be broken down into two primary stages: first, we leverage multi-agent social simulation to generate semantically rich task instructions; second, we employ a multi-level scene generation process to construct the corresponding physically interactive 3D environments. This section provides a detailed walkthrough of each component.

A.1 STAGE 1: SOCIAL SIMULATION FOR TASK INSTRUCTION GENERATION

To avoid generating homogeneous and short-term tasks, we adopt a strategy inspired by MATRIX, performing social simulations within pre-existing embodied scenes to generate meaningful instructions.

The process begins by preprocessing 45 diverse scenes from the Omnidigibson simulation platform. For each scene, we extract key information, including scene images and textual descriptions of room types and unique environmental attributes. This information is fed into a **Role Playing Agent**, which generates plausible character profiles tailored to the scene. For instance, in a house environment, it might simulate a family, defining each member with attributes like name, age, job, relationships, and hobbies.

Next, a **Social Simulation Agent** receives both the character profiles and detailed scene information (e.g., room names and sizes). It then produces tasks that a robot might perform to assist the characters within that social context. A typical generated task might be: “Bring the chess from the counter in the living-room to the table in the garden for dad.”

Finally, to make these language-based instructions machine-executable, a **Summarization Agent** maps the semantic task into the structured BDDL format. This format explicitly defines the goal conditions for the task. During a post-processing phase, we match the objects involved in the task with available 3D assets and use a combination of rule-based filters and a validation agent to eliminate unsupported or duplicate tasks, ensuring the quality and feasibility of the generated data.

A.2 STAGE 2: MULTI-LEVEL SCENE GENERATION

Once a task is defined in BDDL, we need to generate a 3D scene where the initial conditions are met and the task is physically executable. To automate the construction of diverse, multi-room scenes for these long-horizon tasks, we designed an interpretable, multi-level generation framework. The process unfolds across three hierarchical levels: scene, room, and planar.

Scene Level: Object Distribution. To mitigate the complexity of generating a full multi-room scene, we first operate at the scene level. We designed a rule-based **Scene-level Distribution Agent** that takes all objects and initial conditions specified by the task, along with the room layout of a base scene (e.g., room names and sizes). This agent assigns each object and its corresponding state conditions to an appropriate room. The distributor considers task requirements (e.g., if two objects must start on the same table, they are assigned to the same room) while also balancing scene richness and common sense. It prioritizes larger rooms but also considers room function to avoid unnatural clustering or excessive dispersion of objects. After this stage, all objects are assigned to a room and are ready for precise placement.

Room Level: Layout Tree. Within each room, we use a multi-level tree structure to represent the object layout at a coarse granularity. This tree contains two node types: object nodes and relation nodes. The relations are based on nine object state functions supported by Omnidigibson (e.g., *ontop*, *under*, *inside*). If two objects share a spatial relationship, they are connected via a relation node. The tree is built sequentially, with the root node typically being the room’s floor. A **Room-level Organization Agent** is responsible for creating

this structure. It takes the list of objects assigned to the room and a top-down view as input, then outputs a layout tree based on common sense, object sizes, and their approximate positions. For example, it knows a small backpack is more likely to be *ontop* of a table than on the floor. The agent prioritizes satisfying the task’s initial conditions and iteratively refines the tree. If a generated layout proves invalid during placement, the incorrect relation is fed back to the agent as historical context to prevent similar errors in subsequent attempts.

Planar Level: Object constraints in the same plane. This level addresses the challenge of fine-grained placement, particularly for the *ontop* relation. Placing multiple objects on a single surface (like a floor or a large table) using random sampling often results in cluttered, aesthetically unpleasing arrangements that can block a robot’s path.

To solve this, we employ a **Planar-Level Placement Generator**, inspired by recent work, which operates at a finer granularity. For objects placed on the same base surface, this agent establishes precise spatial constraints between them, such as *faceto*, *nextto*, or *alignedwith*. For example, it might specify that a newly placed chair should be *in front of* the desk and *face to* the computer monitor. The optimal position for a new object is found by discretizing the base surface into a grid and selecting the grid cell that maximizes a score derived from these constraints.

Throughout this optimization, two hard constraints are strictly enforced: (1) the new object must not collide with any existing objects, and (2) there must be a valid nearby position for the robot to be spawned, ensuring the object is interactable.

Object Level: Object Placement Sampling. At this level, we use the APIs provided by the Omnigibson system for various relations to sample object positions. This ensures that objects do not collide with other items in the scene while satisfying the positional constraints specified at the Room and Planar levels. The entire implementation is integrated into our **Object-level Sampling Agent**.

After processing all rooms, the complete embodied scene is saved. Finally, we perform a validation step by loading the scene and verifying that a robot can successfully manipulate the task-relevant objects, confirming the task’s executability.

B DETAILED EXPLAINTION OF OUR SCALABLE SIMULATION BACKEND

This appendix provides a detailed technical breakdown of the **Scalable Simulation Backend**, a core component of EmboMatrix. As discussed in the main text, our approach is built on two fundamental principles designed to address the primary bottlenecks in large-scale interactive learning: **semantic abstraction** to accelerate individual physical interactions, and **architectural decoupling** to enable massively parallel rollouts.

The principle of semantic abstraction is concretely implemented through our **Pre-Cached Language-Physics Interface** (detailed in Sec. B.1). This component is responsible for grounding the LLM’s high-level action sequences into low-latency physical state transitions.

Similarly, architectural decoupling is realized by the **Distributed Simulation Backend** (detailed in Sec. B.2). This service-oriented system, composed of a central manager and a fleet of heterogeneous worker nodes, is engineered to manage parallel simulations efficiently and hide system-level overheads.

The following subsections will detail the design and implementation of each of these core components.

B.1 SEMANTIC ABSTRACTION: THE PRE-CACHED LANGUAGE-PHYSICS INTERFACE

A primary performance bottleneck in high-fidelity simulation is the *granularity mismatch* between the LLM’s high-level semantic commands (e.g., `place(apple, table)`) and the simulator’s computationally expensive, low-level micro-dynamics (e.g., contact forces, friction). To resolve this, we designed a structured interface that grounds the LLM’s language outputs into executable state changes in the simulator.

Following a "language in, language out" paradigm, the agent generates a complete program $\pi = [a_1, \dots, a_H]$, where each step a_i is a structured token tuple, $\langle \text{skill}, \arg_1, \dots, \arg_k \rangle$, drawn from a predefined skill library. This design retains the generality of token-level inference while enabling physical grounding through symbolic decomposition. An execution engine interprets this action sequence step-by-step, triggering corresponding low-level controllers.

Crucially, to accelerate this process, we introduce a **pre-cached, outcome-based simulation** mechanism. For common interaction skills whose outcomes are quasi-static (e.g., placing an object), we pre-compute a manifold of valid and physically plausible terminal poses during an offline scene analysis phase. At runtime, once the skill’s preconditions are met (e.g., the robot holds the object near the target), the system bypasses the costly continuous motion simulation and collision resolution entirely. Instead, it directly instantiates a valid outcome from the pre-cached set. This approach preserves the crucial semantic consequences required for the reward signal while accelerating individual skill execution by an estimated **5x to 100x**, making large-scale, closed-loop training in complex environments computationally feasible.

B.2 ARCHITECTURAL DECOUPLING: THE DISTRIBUTED SIMULATION SYSTEM

The second major challenge stems from the conflicting resource requirements of LLM training (typically compute-bound) and large-scale physics simulation (often memory- and graphics-bound). A monolithic architecture that co-locates these processes is inherently inefficient and unscalable. We resolve this by employing an **architecturally decoupled, distributed simulation backend**, as illustrated in Figure 8. This service-oriented design separates the LLM trainer from a heterogeneous pool of simulation workers, allowing each component to run on its specialized, optimal hardware.

This distributed system is composed of three key parts that work in concert to hide latency and maximize throughput.

Heterogeneous Simulator Cluster. A central simulation manager coordinates a distributed pool of worker nodes. These can be dedicated servers, workstations, cloud VMs, or even idle commodity PCs. Each node runs a lightweight daemon that self-registers with the manager, reports its available resources (GPU, VRAM, CPU), and fetches compressed simulation scenarios on demand. Because the simulators operate as independent services requiring no inter-node communication, the system can efficiently leverage globally distributed, commodity hardware, scaling rollout capacity without needing expensive, high-speed interconnects.

Resource-Scheduler. To mitigate the significant latency caused by loading complex scenes, the scheduler acts proactively. At any given training step t , the scheduler polls all worker nodes and inspects the LLM’s dataloader to predict the scenarios needed for future steps $t + 1, \dots, t + k$. It then pre-assigns these future scenarios to idle nodes, which begin pre-loading the required assets. By the time a rollout is dispatched for execution, the corresponding simulation environment is already initialized and "pre-warmed," nearly eliminating loading stalls from the critical path of the training loop.

Task-Dispatcher. Once the agent produces a batch of action sequences, the dispatcher maps each action sequence to its corresponding pre-warmed simulator slot on a worker node. It launches the executions in parallel and streams the resulting experiences back to the learner. As soon as a simulation slot becomes

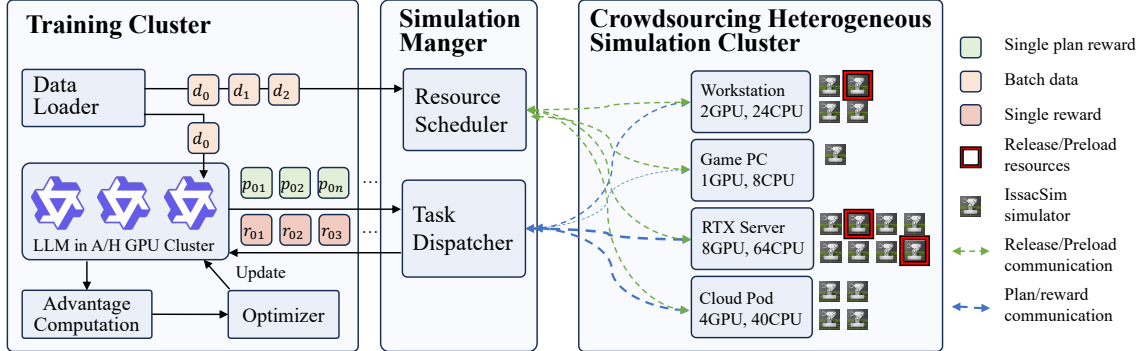


Figure 8: The Architecture of the Distributed Simulation Backend. The LLM trainer generates rollout action sequences and updates its policy via reinforcement learning. A central Simulation Manager schedules these action sequences across a heterogeneous, crowdsourced fleet of simulators. The system strategically overlaps scene loading with execution and streams the resulting experiences (observations, rewards) back to the learner, maximizing hardware utilization.

free, it is immediately reused for the next queued action sequence, ensuring that the simulation hardware remains continuously saturated. This combination of proactive scheduling and dynamic dispatching ensures that wall-clock training time is dominated by the necessary physics simulation itself, rather than by queueing or I/O bottlenecks. This design is what makes our large-scale, physically-grounded LLM training practical, with system overhead accounting for only about 20% of the total training time.

C REWARDS COEFFICIENTS

In our experiments, the agent receives a penalty of -1 if its output action sequence cannot be parsed into a structured format. A base reward of 0.5 is granted for a successfully parsed sequence. The Semantic Relevance reward is scaled by a coefficient $\beta = 0.2$ and is capped at 1. The primary component is the Goal-Oriented Success reward, where the total reward for a task is 30, and the scaling factor α is defined as $30/N_{\text{sub}}$, with N_{sub} being the number of sub-tasks.

D TECHNIQUE APPENDICES

Table 8 enumerates the skill primitives that the agent can compose into high-level programs. Each action takes a structured set of parameters, such as an object index, spatial relation, or target room, allowing the execution engine to translate symbolic action sequences into concrete state transitions. Together, these 13 primitives support navigation, object manipulation, state changes (e.g., open/close, toggle), and basic cooking operations, providing sufficient expressiveness for the long-horizon tasks used in our experiments.

E COMPARATION OF EMBODIED DATA GENERATION

We compare our Multi-Agent-Driven Automated Data Factory with other embodied scene generation works, as shown in Tab 4.



(a) Multi-level layout tree

(b) No multi-level layout tree

(c) LayoutGPT

Figure 9: Comparation of three methods when generating scene of Benevolence_2_int.



(a) Multi-level layout tree

(b) No multi-level layout tree

(c) LayoutGPT

Figure 10: Comparation of three methods when generating scene of Merom_0_garden.

Table 4: Comparison of our work with previous works that can generate interactive 3D scenes and train agents with embodied tasks in 6 aspects. Here, **Fully Automated** refers to the entire process, from embodied task generation to scene generation and RL of the agent, being completed without any human intervention. **Tasks with MASS** means the tasks are generated via multi-agent social simulation frameworks. **Scenes from tasks** means the ability to generate executable embodied scenes for any given task. **Multi room** means tasks executed in a multi-room embodied scene. **Interpretable** means the scene generation process is interpretable. **Self-Verifying** means the generated scene will be verified for completion feasibility.

| Methods | Fully Automated | Tasks with MASS | Scenes from tasks | Multi-room | Interpretable | Self-Verifying |
|-------------|-----------------|-----------------|-------------------|------------|---------------|----------------|
| Behavior-1k | | | | ✓ | ✓ | |
| ProcTHOR | | | | ✓ | ✓ | |
| Holodeck | | | | ✓ | ✓ | |
| Architect | | | | ✓ | | |
| RoboGen | ✓ | | ✓ | | ✓ | |
| Ours | ✓ | ✓ | ✓ | ✓ | ✓ | ✓ |

F EXPERIMENTS DETAILS

We design two LLM-based evaluator for evaluating the generated tasks’ diversity and the aesthetic score of the generated scenes. The two evaluator’s prompts are shown in Tab. 6 and Tab. 7.

There are another two examples of three methods when generating scenes in Fig 9 and 10. We can see that the other two methods – layoutgpt and no layout tree give a messy and infeasible scene.

G LLM USAGE STATEMENT

Large Language Models (LLMs) were used only as auxiliary tools in this work. Specifically, we employed GPT-based models to assist with grammar polishing, wording refinement, and summarization of related works. All core research components—including research ideation, methodology design, experiment execution, and result analysis—were conducted entirely by the authors. No LLM contributed at a level that would merit authorship.

Table 5: Examples of task generation with/without social simulation in Scene Beechwood_0_garden

| With Social Simulation | Without Social Simulation |
|--|--|
| Pick up the basketballs in gym_0 and place them in the equipment rack in locker_room_0. | Please pick up the basketball from the storage rack in the gym_0 and place it on the mat in the gym_0. |
| Bring the yoga mats from locker_room_0 to gym_0 for Ms. Clara's yoga class. | Pick up the water bottle from the bench in locker_room_0 and place it inside the cabinet in locker_room_0. |
| Pick up the smoothie blender from corridor_0 and place it on the table in locker_room_0 for Ms. Clara's smoothie workshop. | Go to bathroom_0, toggle on the hand dryer, then toggle off the hand dryer after 20 seconds. |
| Gather sports bottles from corridor_1 and corridor_2 and place them in gym_0 for Coach Alex's basketball practice. | Pick up the volleyball from the storage box in locker_room_1 and place it on the counter in corridor_2. |
| Collect towels from locker_room_1 and distribute them in bathroom_0 for students to use after practice. | Open the locker in locker_room_1, pick up the towel inside, and place it on top of the bench in locker_room_1. |
| Pick up cleaning supplies from bathroom_0 and clean the floors in corridor_0 and corridor_1. | Pick up the gym bag from the bench in locker_room_0 and place it inside the storage cabinet in corridor_1. |
| Place the cones from corridor_2 in gym_0 for Coach Alex's basketball drills. | Go to gym_0, pick up the whistle from the referee table, and place it on the counter in corridor_0. |
| Toggle on the fans in gym_0 to ensure ventilation during Coach Alex's practice session. | Toggle on the light switch in corridor_2, then toggle off the light switch after 10 minutes. |
| Put the foam rollers from locker_room_1 inside locker_room_0 for Ms. Clara's wellness activities. | Pick up the cleaning spray from the shelf in corridor_0 and place it on top of the counter in bathroom_0. |
| Close the windows in corridor_0 to maintain temperature during Ms. Clara's fitness workshop. | Pick up the shoes from the floor in locker_room_1 and place them inside the shoe cabinet in locker_room_1. |

Table 6: **Prompt for the gpt4-based task diversity evaluator.**

Please analyze the diversity of the following generated commands and provide a score out of 10 based on the following criteria:

1. **Variety:** Do the commands include a diverse range of actions, objects, and scenarios? Do the commands cover different types of actions (e.g., picking up, placing, toggling) and involve various objects and locations? However the robot can only take concrete actions, such as pick up, move, toggle, place and so on, so don't be too strict about the action diversity.
2. **Inclusion of Specific Characters:** Do the commands explicitly mention specific individuals (their name or roles)? The characters number is limited to 2-4. Are the commands tailored to these characters, and do they reflect their unique roles or characteristics? If the commands don't include specific characters, please give a low score.

You need to be careful, just focus on the given criteria. After analyzing the commands, give your section scores and an overall score, provide a detailed explanation for the score.

Here are the commands: {commands}

Table 7: **Prompt for the gpt4-based scene aesthetic evaluator.**

You are a professional scene arrangement evaluator, capable of providing objective assessments of the reasonableness and aesthetics of each scene. Now, to complete a task, the user needs to place some new objects in an initial room, and these objects must satisfy certain spatial relationships, such as "A inside B" meaning B must be placed inside A, and so on. In the context of this task, please act as an evaluator to assess how well the user has arranged these new objects.

We will provide you with an image, which is a top-down view of a room. The image will label the names of some objects, which are either newly added objects or initial objects that have spatial relationships with the newly added ones. Unlabeled objects are part of the room's original arrangement. Additionally, we will provide a JSON description of the new added objects that must be placed in this room, along with their spatial relationships that must be satisfied.

Here are some rules you must follow:

Step 1: Start with a full score of 10.

then:

1. Check Label Correspondence (Deduct 0–2 points)

- Verify whether the bounding boxes in the image match the objects specified in the JSON file.

- If there are mismatches, omissions, or incorrect names, deduct points accordingly:

- Minor mismatches (1–2 objects incorrect): Deduct 1 point

- Major mismatches (multiple objects incorrect or serious relational errors): Deduct 2 points

2. Assess Room Clutter (Deduct 0–4 points)

- Observe whether the room looks cluttered, whether objects are overlapping, crowded, or arranged chaotically.

- Deduct points as follows:

- Generally tidy, only slightly crowded: Deduct 1 point

- Noticeable crowding or some overlap: Deduct 2 points

- Multiple overlaps or moderate chaos but still recognizable: Deduct 3 points

- Extremely cluttered or unrecognizable: Deduct 4 points

3. Evaluate Aesthetics and Placement Reasonableness (Deduct 0–4 points)

- Consider whether objects are oriented naturally, placed reasonably, and visually harmonious.

- Deduct points as follows:

- Mostly reasonable with minor visual inconsistencies: Deduct 1 point

- Some objects have unnatural orientation or awkward positions: Deduct 2 points

- Several unreasonable placements or orientations: Deduct 3 points

- Most objects poorly placed or visually chaotic: Deduct 4 points

Object Placements and Relationships: {new_added_tree}

Please provide the score and a short explanation.

Table 8: List of available action primitives and their parameters

| Action | Parameters |
|--------------------------|--|
| move | {object_index: n } |
| turn | {yaw: y } |
| pick_up | {object_index: n } |
| place | {object_index: n , relation: r } |
| move_forward | {distance: x , yaw: y } |
| open | {object_index: n } |
| close | {object_index: n } |
| toggle_on | {object_index: n } |
| toggle_off | {object_index: n } |
| heat_object_with_source | {object_index: n , source_index: m } |
| cook_object_with_tool | {object_index: n , source_index: m } |
| froze_object_with_source | {object_index: n , source_index: m } |
| go_to_room | {room_name: s } |